DEMONSTRATION OF THE THERMOGRAPHIC PHOSPHOR HEAT-TRANSFER TECHNIQUE AS APPLIED TO AERODYNAMIC HEATING OF EXTERNAL STORES

S. S. Baker, et al

Arnold Engineering Development Center
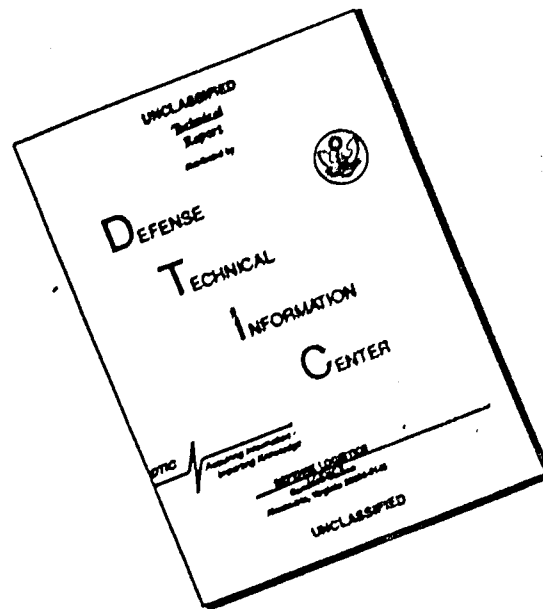Arnold Air Force Station, Tennessee

November 1973

DISCLAIMER NOTICE

THIS DOCUMENT IS BEST QUALITY AVAILABLE. THE COPY FURNISHED TO DTIC CONTAINED A SIGNIFICANT NUMBER OF PAGES WHICH DO NOT REPRODUCE LEGIBLY.

AD-769306

DOCUMENT CONTROL DATA - R & D		
(Security classification of title, body of abstract and indexing annotation must be entered when the overall report is classified)		
1. ORIGINATING ACTIVITY (Corporate author) Arnold Engineering Development Center Arnold Air Force Station, Tennessee 37389	2a. REPORT SECURITY CLASSIFICATION UNCLASSIFIED	
	2b. GROUP N/A	

3. REPORT TITLE

DEMONSTRATION OF THE THERMOGRAPHIC PHOSPHOR HEAT-TRANSFER TECHNIQUE
AS APPLIED TO AERODYNAMIC HEATING OF EXTERNAL STORES

4. DESCRIPTIVE NOTES (Type of report and inclusive dates)
Final Report - January 30,1973

5. AUTHOR(S) (First name, middle initial, last name)

S. S. Baker and R. K. Matthews, ARO, Inc.

6. REPORT DATE November 1973	7a. TOTAL NO. OF PAGES ~~49~~ 41	7b. NO. OF REFS 6
8a. CONTRACT OR GRANT NO.	9a. ORIGINATOR'S REPORT NUMBER(S) AEDC-TR-73-128 AFATL-TR-73-154	
b. PROJECT NO.		
c. Program Element 62602F	9b. OTHER REPORT NO(S) (Any other numbers that may be assigned this report) ARO-VKF-TR-73-76	
d.		

10. DISTRIBUTION STATEMENT

Approved for public release; distribution unlimited.

11. SUPPLEMENTARY NOTES Details of illustrations in this document may be better studied on microfiche. Available in DDC	12. SPONSORING MILITARY ACTIVITY Air Force Armament Laboratory/DLGC Eglin Air Force Base Florida 32542

13. ABSTRACT   The purpose of this investigation was to design and conduct a
wind tunnel test which demonstrated the feasibility of applying wind
tunnel techniques to the aerodynamic heating problems encountered in the
supersonic carriage of external stores. The test incorporated the
thermographic phosphor paint technique on an MK-84 store attached to the
left inboard pylon of a 0.05-scale model of the F-4C. The test was made
at nominal free-stream Mach numbers of 1.49, 1.76, 2.00, and 2.50; at
nominal free-stream unit Reynolds numbers between 3.67×10^6 and 4.64×10^6 ft^{-1}; and at aircraft angles of attack of 0 and +4 deg. Typical
heat-transfer-rate distributions on the MK-84 are presented. Thermo-
graphic Datacolor photographs are also included showing characteristic
heating patterns on the external store and significant variations in the
heat transfer coefficient at various X/L locations caused by local "hot
spots." Other photographic data illustrate the complexity of the flow
field around the store.

DD FORM 1473 NOV 65

i

KEY WORDS	LINK A		LINK B		LINK C	
	ROLE	WT	ROLE	WT	ROLE	WT
external stores						
aerodynamic heating						
supersonic flow						
temperature measuring instruments						
heat transfer						
phosphorescent materials						
F-4C aircraft						
MK-84 bombs						
fuel tanks						
wind tunnel tests						

NOTICES

ACCESSION for

NTIS	White Section	☑
C	Buff Section	☐
UN CED		☐
JUSTIFICATION		

BY

DISTRIBUTION/AVAILABILITY CODES

Dist.	AVAIL. and/or SPECIAL
A	

ib

DEMONSTRATION OF THE THERMOGRAPHIC PHOSPHOR HEAT-TRANSFER TECHNIQUE AS APPLIED TO AERODYNAMIC HEATING OF EXTERNAL STORES

S. S. Baker and R. K. Matthews
ARO, Inc.

FOREWORD

The work reported herein was conducted by the Arnold Engineering Development Center (AEDC), Air Force Systems Command (AFSC), under the sponsorship of the Air Force Armament Laboratory (AFATL), Eglin Air Force Base, Florida, under Program Element 62602F.

The results presented herein were obtained by ARO, Inc. (a subsidiary of Sverdrup & Parcel and Associates, Inc.), contract operator of AEDC, AFSC, Arnold Air Force Station, Tennessee. The test was conducted on January 30, 1973, under ARO Project No. VA296, and the data package was completed on April 17, 1973. The manuscript was submitted for publication on June 12, 1973.

The authors wish to express their appreciation to Messrs. L. D. Carter and E. C. Knox of the von Kármán Gas Dynamics Facility for their advice during the testing phase of this program and during the preparation of the report.

This technical report has been reviewed and is approved.

JIMMY W. MULLINS
Lt Colonel, USAF
Chief Air Force Test Director, VKF
Directorate of Test

FRANK J. PASSARELLO
Colonel, USAF
Director of Test

ABSTRACT

The purpose of this investigation was to design and conduct a wind tunnel test which demonstrated the feasibility of applying wind tunnel techniques to the aerodynamic heating problems encountered in the supersonic carriage of external stores. The test incorporated the thermographic phosphor paint technique on an MK-84 store attached to the left inboard pylon of a 0.05-scale model of the F-4C. The test was made at nominal free-stream Mach numbers of 1.49, 1.76, 2.00, and 2.50, at nominal free-stream unit Reynolds numbers between 3.67×10^6 and 4.64×10^6 ft^{-1}; and at aircraft angles of attack of 0 and +4 deg. Typical heat-transfer-rate distributions on the MK-84 are presented. Thermographic Datacolor photographs are also included showing characteristic heating patterns on the external store and significant variations in the heat-transfer coefficient at various X/L locations caused by local "hot spots." Other photographic data illustrate the complexity of the flow field around the store.

CONTENTS

APPENDIXES

I. ILLUSTRATIONS

Figure

NOMENCLATURE

BL — Buttock line from plane of symmetry, in.

C_p — Specific heat of air at constant pressure, Btu/lbm-°R

ΔE — Measured voltage of Gardon gage

FS — Fuselage station, in.

h — Heat-transfer coefficient, $\dot{q}/T_{aw} - T_w$, Btu/ft²-hr-°R

L — MK-84 store model length, 7.83 in.

M_∞ — Free-stream Mach number

p_o — Tunnel stilling chamber pressure (stagnation pressure), psia

$\dot{q}$ — Heat-transfer rate, Btu/ft²-hr

R — Radius, measured from and normal to model longitudinal centerline, in.

Re_L — Free-stream Reynolds number based on store length (12.83 ft for flight, 0.652 ft for wind tunnel)

Re_∞/ft — Free-stream unit Reynolds number, ft⁻¹

SF	Gardon gage scale factor
St	Stanton number, $\dot{q}/\rho_\infty V_\infty (H_{aw} - H_w)$
T_{aw}	Model adiabatic wall temperature, °R
T_e	Edge temperature of Gardon gage, °R
T_i	Initial model wall temperature; model wall temperature before exposure to tunnel flow, °R
T_0	Tunnel stilling chamber temperature (stagnation temperature), °R
T_w	Model wall temperature, °R
$T_{w_{gage}}$	Effective wall temperature as sensed by the Gardon heat-transfer-rate gage, °R
ΔT	Temperature difference from the center to the edge of the Gardon gage
Δt	Exposure time of model to free-stream airflow, sec
V_∞	Free-stream velocity, ft/sec
X	Longitudinal centerline distance for MK-84 store model, in.
α	Parent body angle of attack, deg
ρ_∞	Free-stream density, slugs/ft³
$\sqrt{\rho c k}$	Material property parameter, Btu/ft²-sec½-°R (density ρ, specific heat c, conductivity k)
ϕ	Parent body roll angle, deg
ϕ_{ray}	Circumferential position on MK-84 store model, deg

SUBSCRIPTS

ft	Flight conditions
wt	Wind tunnel conditions

SECTION I
INTRODUCTION

In December of 1971, Epstein (Ref. 1) presented a paper at the Aircraft/Stores Compatibility Symposium in which he discussed supersonic carriage of conventional weapons. Some of the important conclusions to be drawn from that paper are: (1) many supersonic aircraft/store combinations are speed "limited" by store aerodynamic heating, (2) flight test evaluation of all aircraft/store situations is not possible, and (3) the complexity of the aircraft/store flow environment defies analytic description.

Figure 1[1] (Appendix I) illustrates how the performance envelope of a typical present-day aircraft has been severely limited by external store heating. Unfortunately, these limitations are sometimes imposed by "arbitrary temperature limits[2] on the store." Almost all present-day bombs and fuses have, as their explosive charge, some form of TNT which melts at about 178°. When this explosive melts, it becomes unstable and very dangerous. However, to determine the actual temperature of the TNT in flight one must know the following:

1. The maximum temperature attainable at the specific flight condition (i.e., T_{aw}), see Fig. 1;

2. The rate at which heat is transferred to the store; and

3. The length of time at a given flight condition.

Of these three, the heat-transfer rate is by far the hardest to determine. As a result, the adiabatic wall temperature (T_{aw}) is often used as a conservative limit.

Some analytic work has been done on store heating, for example, under a contract with Eglin AFB, the Armour Research Foundation performed extensive calculations of store heating distributions for the case of a MARK 83 bomb in an interference-free flow field (Ref. 2). Of course, the actual flow field is far from interference-free as will be shown later in this report.

The purpose of this investigation was to design and conduct a wind tunnel test which demonstrated the feasibility of wind tunnel testing techniques as applied to the store aerodynamic heating problem. The store thermal environment was obtained using the thermographic phosphor paint technique. The phosphor data provide a complete thermal mapping of the heat-transfer coefficient distributions for wind tunnel conditions. If proper scaling laws are known, these heat-transfer-rate distributions can be extrapolated to flight

---

[1] A similar figure was presented in Ref. 1.

[2] It should be emphasized that other factors may also restrict the performance envelope, but this report is directed toward techniques to better define the store temperature limitations.

conditions. Then, with the aid of existing heat conduction computer codes, the heat-transfer distributions for flight conditions can be incorporated with aircraft flight envelopes to provide realistic store temperatures for flight. This could significantly improve the current aircraft operating limits with external stores and help to provide a "total force....operating at near the design speed of the aircraft."[3]

The test was conducted in the von Kármán Gas Dynamics Facility (VKF) 40-in. Supersonic Wind Tunnel (A) at Mach numbers of 1.49, 1.76, 2.00, and 2.50, and nominal free-stream unit Reynolds numbers from 3.67×10^6 to 4.64×10^6/ft. A 0.05-scale MK-84 was used as the external store and an existing F-4C model was used to simulate the flow field of the parent body. The parent model orientations consisted of angles-of-attack of 0 and +4 deg. Two basic configurations were tested:

F-4C/MK-84/WITH FUEL TANKS

F-4C/MK-84/WITHOUT FUEL TANKS.

SECTION II
APPARATUS

2.1 WIND TUNNEL

Tunnel A is a continuous, closed-circuit, variable density wind tunnel with an automatically driven flexible-plate-type nozzle and a 40- by 40-in. test section. The tunnel can be operated at Mach numbers from 1.5 to 6 at maximum stagnation pressures from 29 to 200 psia, respectively, and stagnation temperatures up to $750°R$ ($M_\infty = 6$). Minimum operating pressures range from about one-tenth to one-twentieth of the maximum at each Mach number. Tunnel A has a model injection system which makes it possible to change model configurations without interrupting the tunnel flow (Fig. 2). A description of the tunnel and airflow calibration information may be found in Ref. 3.

2.2 MODELS

A photograph showing the F-4C parent model with the MK-84 and fuel tank mounted is presented in Fig. 3. Only the MK-84 bomb mounted on the inboard pylon of the left wing was instrumented.

The 0.05-scale MK-84 store was fabricated at the VKF. The store model was constructed of C-7 epoxy because of its low thermal conductivity which is required for the thermographic phosphor paint technique. In addition to the thermographic paint, the store was instrumented with a Gardon heat-transfer-rate gage and two wall temperature gages. Model details and instrumentation locations are shown in Fig. 4. It should be noted that the MK-84 store was at a 1-deg angle of incidence in the carriage position.

---

[3]Comment at Tactical Fighter Symposium expressing the desires of General William Momyer, TAC Commander.

2

A sketch illustrating the relative size of the F-4C, MK-84, and fuel tank is presented in Fig. 5, and the two pylon stations on each wing are indicated.

2.3 INSTRUMENTATION

2.3.1 Thermographic Phosphor Paint

Thermographic phosphorescence is the emission of luminescent light having temperature-dependent intensity that decreases exponentially with increasing temperature. The paint phosphorescence is activated by ultraviolet (UV) light, and the intensity of emission[4] depends on the properties of the particular phosphorescent paint and the energy of the activating ultraviolet light, as well as the temperature. A plot of the emission brightness for the phosphor used in this test is given in Fig. 6 as a function of temperature; the intensity of the ultraviolet lights for this test was nominally 2.8 ultraviolet light units (280 μw/cm^2).

The technique for obtaining the model surface temperature patterns at the desired test conditions consists of photographing the painted model surface and measuring the optical density (brightness) of the recorded image. The measured film density is related to the model surface temperature, which can be related to the surface aerodynamic heat-transfer coefficient as will be discussed later.

The model phosphorescence photographs were obtained using Beattie-Coleman Varitron® 70-mm sequence cameras set at f/4 and 0.5-sec exposure times. Eastman Kodak Tri-X Pan® film was developed using the Eastman Kodak Versamat® process.

2.3.2 Heat-Transfer-Rate Gage and Wall Temperature Gages

A Gardon heat-transfer-rate gage and two wall temperature gages were used to monitor heating rates on the model. Their physical locations on the model were shown in Fig. 4. The heat-transfer-rate gage operates on the Gardon gage principle (Ref. 4), and a sketch of a typical gage is shown on the right-hand side of Fig. 7.

The two wall temperature gages operate on the basic thermocouple principle with the two dissimilar metal-wire leads divided into very fine "whiskers." This was done to reduce conduction losses. A sketch of the basic construction of a wall temperature gage is shown on the left-hand side of Fig. 7. Unfortunately, conduction losses were not eliminated, and the gage readings were observed to be consistently low ($\sim$7°F). For this reason, data from the two wall temperature gages were not used in the data reduction.

---

[4]In order to provide a good reflective background for the phosphor paint, the model was painted white before the phosphor paint was applied.

SECTION III
PROCEDURE

3.1 TEST CONDITIONS AND PROCEDURE

3.1.1 Test Conditions

The nominal tunnel operating conditions were as follows:

M_∞	p_0, psia	T_0, °R	ρ_∞, s ug/ft³	V_∞, ft/sec	Re_∞/ft, ft⁻¹
1.49	15.0	638	7.88×10^{-4}	1535	3.67×10^6
1.76	17.0	638	6.71×10^{-4}	1712	3.84×10^6
2.00	21.1	639	6.37×10^{-4}	1846	4.29×10^6
2.50	29.2	638	5.05×10^{-4}	2063	4.64×10^6

A complete test summary is presented in Table I (Appendix II).

3.1.2 Test Procedure

The test sequence consisted of injecting the model into the airstream, translating it forward to the test section, and taking four photographs of the model at 4-sec intervals. The model was exposed to the airflow about 10 sec before reaching the test section, and the model remained in the test section for approximately 16 to 18 sec. The model was cooled to about 70 to 80°F prior to each injection. The Gardon gage heat sink temperature and the model wall temperatures were monitored during the cooling cycle to ensure a uniform temperature distribution before a subsequent injection was made.

The outputs from the two wall temperature gages and the Gardon heat-transfer gage were recorded continuously from before the model injection until the beginning of the retract cycle. The recordings were made on magnetic tape with a Beckman 210 analog-to-digital converter, each channel being sampled every 0.05 sec during the recording interval. Indicate bits marked the time sequence of such events as model arrival on centerline, model arrival at test section position, and the times at which the photographs were taken.

Because of the obstructed side view of the instrumented model by the other stores and because of the desirability of having the Gardon gage visible in each photograph (for establishing reference levels in the phosphor paint data), the parent body model was rolled ±45 deg as illustrated in Fig. 8. Two cameras were used (one on each side of the tunnel) so that the heating patterns could be photographed from both the inboard and outboard positions by rolling the model -45 and +45 deg, respectively. A typical black/white picture of the phosphor-painted store with the parent body rolled +45 deg is shown in Fig. 9.

3.2 DATA REDUCTION

The aerodynamic heat-transfer coefficient at the Gardon gage location was computed by

$$h_{wt} = \frac{\dot{q}}{T_{aw} - T_{w_{gage}}} \tag{1}$$

where the heat-transfer rate ($\dot{q}$) and the effective wall temperature ($T_{w_{gage}}$) of the Gardon gage were obtained as follows

$$\dot{q} = (SF)(\Delta F) \tag{2}$$

and

$$T_{w_{gage}} = T_e + 0.75(\Delta T) \tag{3}$$

The Stanton number was computed as

$$St_{wt} = \frac{h_{wt}}{\rho_{\infty_{wt}} V_{\infty_{wt}} C_p} \tag{4}$$

where the specific heat of air at constant pressure (C_p) was assumed to be 0.240 Btu/lbm-°R.

Because of possible nonuniformities in either the phosphor coating or the incident ultraviolet light (for example, shadows caused by model geometry), pretest pictures of the model were obtained in the test section under the same conditions (but without the tunnel running) that existed for the test pictures. By subtracting the measured optical density of the pretest picture from the corresponding test picture, the influence of these nonuniformities was eliminated from the final results. In other words, the black/white picture that is analyzed is the difference between the test picture positive and a negative of the pretest picture. The superposition of these two pictures yields the difference in density between them. This difference in film density as shown in Fig. 10a represents the change in temperature between the test conditions and the pretest condition.

Data reduction of the film density patterns was accomplished using a Datacolor 703-32® analyzer. The Datacolor system uses a black/white television (TV) camera to produce a standard TV signal, or image, of the test picture. A digital video processor analyzes the shades of gray in the TV image and classifies them into increments or shades of gray (twelve increments were used in the present analysis). A different color is assigned to each increment, and the appropriate color TV signal is generated by the digital processor. These signals are then displayed on a color monitor unit. The color photograph corresponding to Fig. 10a is presented in Fig. 10b. Each color in this photograph corresponds to a specific model wall temperature range.

The conversion from model wall temperature ranges to aerodynamic heat-transfer coefficient (h_{aw}) is accomplished by assuming that the wall temperature response is similar to that of a semi-infinite slab. It should be pointed out that the level of the wall temperatures inferred from the phosphor paint was adjusted to agree with those inferred from the Gardon gage. The heat conduction equation for the wall temperature rise of a semi-infinite slab is

$$\frac{T_w - T_i}{T_{aw} - T_i} = 1 - e^{\beta^2} \, \text{erfc}\, \beta \tag{5}$$

where

$$\beta = \frac{h_{aw}\sqrt{\Delta t}}{\sqrt{\rho c k}}$$

The adiabatic wall temperature (T_{aw}) can be shown to be equal to about $0.95\ T_o$. The initial wall temperature (T_i) and the stagnation temperature (T_o) were obtained from the recordings of the Beckman 210 analog-to-digital converter. The wall temperature ranges from the color photograph are substituted into the left-hand side of Eq. (1) so that values of β can be determined. Thus,

$$h_{aw} = \frac{\beta\sqrt{\rho c k}}{\sqrt{\Delta t}} \tag{6}$$

The material property parameter ($\sqrt{\rho c k}$) was determined to be 0.030 Btu/ft²-sec$^{1/2}$-°R for the MK-84 model material (C-7 epoxy), and Δt is the exposure time to the airflow.

3.3 DATA PRECISION

Uncertainties (bands which include 95 percent of the calibration data) in the basic tunnel parameters (p_o, T_o, and M_∞) were estimated from repeat calibrations of the instrumentation and from the repeatability and uniformity of the test section flow during tunnel calibrations. These uncertainties were then used to estimate uncertainties in other free-stream properties using the Taylor series method of error propagation. The results are tabulated below:

| Nominal M_∞ | Uncertainty ($\pm$), percent | | | | | |
	M_∞	p_∞	T_∞	ρ_∞	V_∞	Re_∞/ft
1.49	0.7	0.5	0.9	1.5	0.7	1.3
1.76	0.7	0.5	0.9	1.7	0.6	1.4
2.00	0.5	0.5	0.9	1.5	0.5	1.4
2.50	0.3	0.5	0.9	1.3	0.5	1.4

Measurements of model attitude in pitch and roll are precise within ±0.05 and ±0.1 deg, respectively, based on repeat calibrations.

The estimated precision of the heat-transfer coefficient levels for the Gardon gage and the Datacolor system are:

Parameter	Uncertainty (±), percent
$h_{Gardon\ Gage}$	12
$h_{Datacolor}$	39

The relatively large values for these uncertainties is directly attributable to the low driving potential $(T_{aw} - T_w)$ that existed for the present test. The F-4C parent model used for this test was restricted to a maximum stagnation temperature of 180°F. Normally, the tunnel A stagnation temperature would be about 50°F higher which would substantially reduce the uncertainties quoted above. It should also be mentioned that the above values are based only on uncertainties of measured parameters and do not include uncertainties which may be attributable to violations of the semi-infinite slab assumptions. It should be emphasized, however, that local variations in the heat-transfer coefficient were clearly discernible in the data, and "hot spots" were easily detected.

SECTION IV
RESULTS AND DISCUSSION

4.1 WIND TUNNEL RESULTS

In Epstein's paper (Ref. 1), the restrictions imposed on aircraft store combinations by "arbitrary" temperature limitations were discussed. At that time, there were no acceptable techniques for determining realistic store temperatures at low supersonic speeds other than flight-test representative cases. The color photograph presented in Fig. 10 shows heat-transfer coefficients on an external store obtained at simulated conditions in a wind tunnel by application of the thermographic phosphor technique. This demonstrates the feasibility of using this technique for the store aerodynamic heating problem.

Additional Datacolor photographs obtained on the outboard side of the MK-84 are presented in Fig. 11. These photographs compare the "fuel tank on" heating patterns on the MK-84 with the "fuel tank off" patterns. One might expect that the fuel tank bow shock impingement on the outboard side of the MK-84 would produce a local "hot spot." Close inspection of the photographs does, in fact, show localized "hot spots" for the "fuel tank on" configuration. The fuel tank bow shock impingement is substantiated by the shadowgraph picture presented in Fig. 12, which shows that the location of the shock impingement on the MK-84 is approximately the same as that of the "hot spots" shown in Fig. 11. The photographs shown in Figs. 10 and 11 vividly illustrate that the Datacolor analysis of the thermographic-phosphor paint data can provide good quantification of the thermal environment of an external store.

In Fig. 13a, data comparisons are again made between "fuel tank on" and "fuel tank off" heating distributions for the outboard side of the MK-84 (inboard distributions are given in Fig. 13b). However, in this case, the data are presented as axial distribution plots for a single radial position (i.e., ϕ_{ray} = 135 deg). These distributions were obtained by making data fairings from the corresponding Datacolor photographs for ϕ_{ray} = 135 deg. By noting the axial location of the various color changes, the relative heating levels were determined along the model. In addition, the relative slope of the heating distribution at each color change can be determined by observing which color corresponds to the higher temperature. However, a comparison of these axial distribution plots with the color photographs of Figs. 10 and 11 clearly shows the advantage of the latter form of data presentation.

Additional axial distribution data fairings are presented in Figs. 14 and 15. These data show the influence of angle of attack and radial position for the specific conditions listed. There are large variations with radial position (Fig. 15) as the flow field is obviously not axisymmetric. More information regarding the flow field and surface streamlines can be obtained by examination of oil flow photographs. During the present test, a limited number of oil flow photographs were obtained, and a representative one is presented in Fig. 16. Here again, the flow field complexity is vividly illustrated.

4.2 APPLICATION OF WIND TUNNEL RESULTS TO FLIGHT CONDITIONS

In Section 1, it was implied that the heat-transfer coefficients determined at the simulated conditions in the wind tunnel could be used to provide realistic store temperatures for flight conditions. The schematic presented in Fig. 17 illustrates the procedures for accomplishing this, and the table below provides a "status report" of each item.

Item	Status
Heat-transfer rates measured in wind tunnel	Feasibility demonstrated by this report
Flight conditions	Function of a given mission
Aerodynamic scaling laws	Can be determined by correlation of flight and wind tunnel data (tentative program currently in planning stage)
Heat-transfer rates for flight conditions	Function of specific configuration and mission
Computer code for store heat conduction	Available at AEDC (Ref. 5); checkout runs complete
Temperature distribution on store (flight)	State-of-the-art technology available to perform task

As can be seen, the determination of the proper aerodynamic scaling laws is the area where future efforts should be directed. A hypothetical determination of the proper aerodynamic scaling laws can be obtained by assuming that a turbulent boundary layer exists for both the flight and wind tunnel conditions. For turbulent boundary layers on simple geometries, it can be shown (Ref. 6) that

$$St(Re_1)^{1/5} = const \tag{7}$$

To illustrate the application of scaling laws this relationship was used to extrapolate the present data to flight conditions. It should be emphasized that this extrapolation technique may or may not be applicable. To substantiate this procedure a direct correlation between flight test data and wind tunnel data should be made.

Equation (7) can be written as

$$\left[St(Re_1)^{1/5}\right]_{fl} = \left[St(Re_1)^{1/5}\right]_{wt} \tag{8}$$

which reduces to

$$St_{fl} = St_{wt}\left[\frac{Re_1_{wt}}{Re_1_{fl}}\right]^{1/5} \tag{9}$$

where St_{fl} is defined as

$$St_{fl} = \frac{h_{fl}}{\rho_{\infty fl} V_{\infty fl} C_p} \tag{10}$$

Rearranging Eq. (10) gives

$$h_{fl} = St_{fl} \rho_{\infty fl} V_{\infty fl} C_p \tag{11}$$

The present Mach 2.0 wind tunnel data have been extrapolated to flight conditions at 20,000 ft, and these results are shown in Fig. 18. Also shown in Fig. 18 is a heating rate distribution obtained from Ref. 2. This theoretical distribution was based on an interference-free flow field at $M_\infty = 2.0$. Note that the theoretical calculations were as much as 100 percent below the data during of the present test. This emphasizes the fact that the complexity of the aircraft/store flow environment defies analytical description.

In Ref. 2, heating-rate distributions were presented for altitudes from 0 to 100,000 ft. Extrapolation of the wind tunnel data to various altitudes by the above procedures is illustrated in Fig. 19. The implicit assumption in this extrapolation is that the heating rate distribution is not a function of Reynolds number for a turbulent boundary layer.

SECTION V
CONCLUSIONS

Aerodynamic heating tests were conducted on an MK-84 bomb model mounted on the left inboard pylon of a 5-percent-scale model of the F-4C. The test was run at nominal free-stream Mach numbers of 1.49, 1.76, 2.00, and 2.50. Complete thermal mappings were obtained by the thermographic-phosphor paint technique. Based on an analysis of these data, the primary conclusions are:

1. This investigation has demonstrated the feasibility of applying a wind tunnel testing technique to the store aerodynamic heating problem.

2. Thermal mappings indicate that the local "hot spots" produced significant variations in the heat-transfer coefficient at various X/L locations.

3. Photographic data clearly illustrate the complexity of the flow field around the store and interference-free calculations can be 100 percent below the measured values.

4. The Datacolor analysis of the thermographic-phosphor paint data provided good quantification of the thermal environment of an external store.

REFERENCES

1. Epstein, Charles S. "Supersonic Delivery of Conventional Weapons - Fact or Fancy?" Aircraft/Stores Compatibility Symposium, AFFDL-TR-72-67, Vol. 1, pp. 51-72, August 1972.

2. Budemholzer, R. A., Goldsmith, A., and Nielsen, H. J. "Investigation of Problems of Temperature and Pressure Influencing the Design of Bomb Weapons." AFAC-TR-57-112 (I), November 1957.

3. Coats, J.D. and Pfaff, L. J. "Flow Characteristics of the VKF/AEDC 40-inch Supersonic Wind Tunnel." AEDC-TR-66-189 (AD376952L), November 1966.

4. Gardon, Robert. "An Instrument for the Direct Measurement of Intense Thermal Radiation." The Review of Scientific Instruments, Vol. 24, No. 5, pp. 366-370, May 1953.

5. Rochelle, James Kenneth. "TRAX-A Finite Element Program for Transient Heat Conduction Analysis of Axisymmetric Bodies." Masters Thesis, University of Tennessee Space Institute, March 1973.

6. Harms, R. J., Schmidt, C. M., Harawalt, A. J., and Schmitt, D. A. "A Manual for Determining Aerodynamic Heating of High-Speed Aircraft." Bell Aircraft Corporation, Report No. 7006-3352-001 (AD229434), June 1959.

APPENDIXES
I. ILLUSTRATIONS
II. TABLES
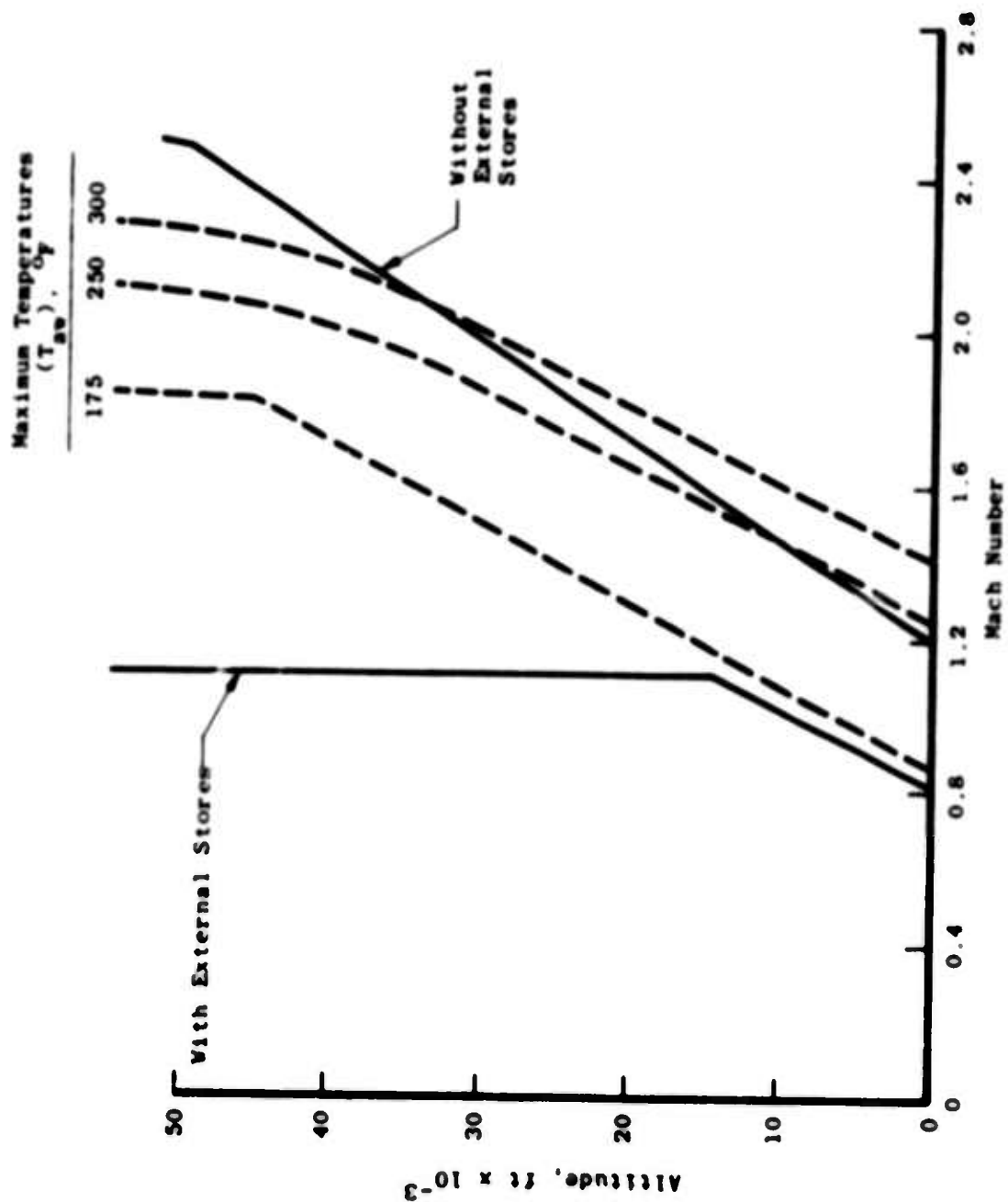
Fig. 1 Performance Envelope of Present-Day Aircraft
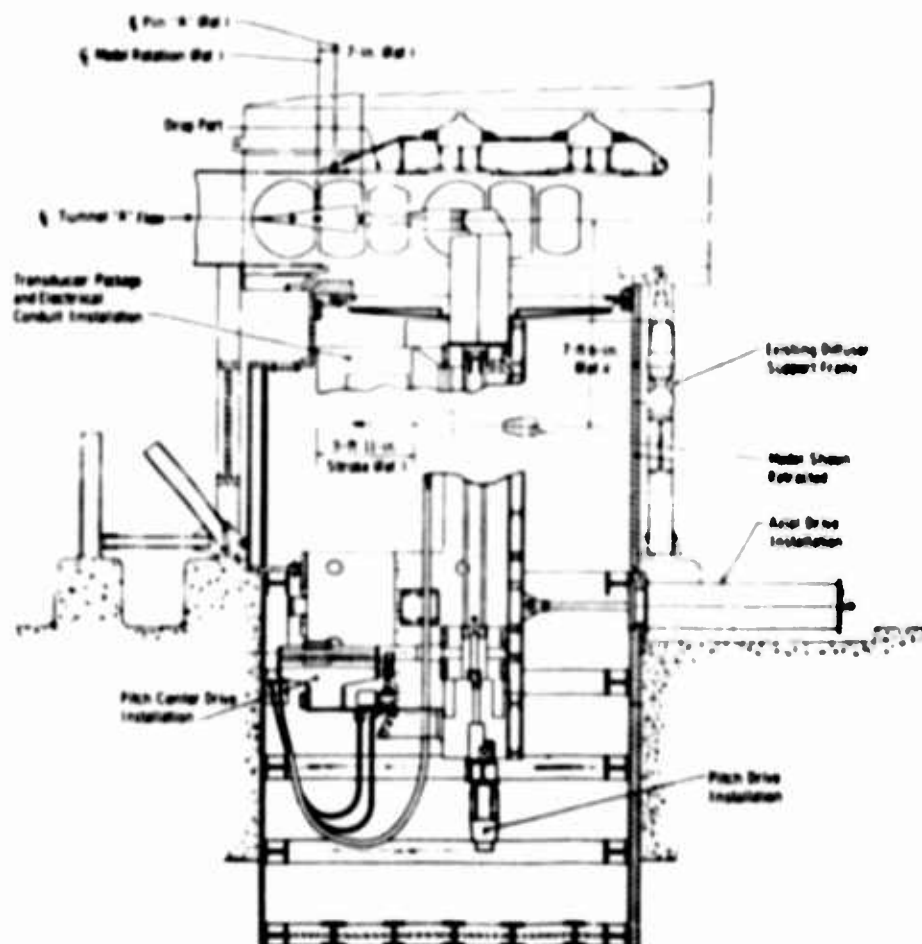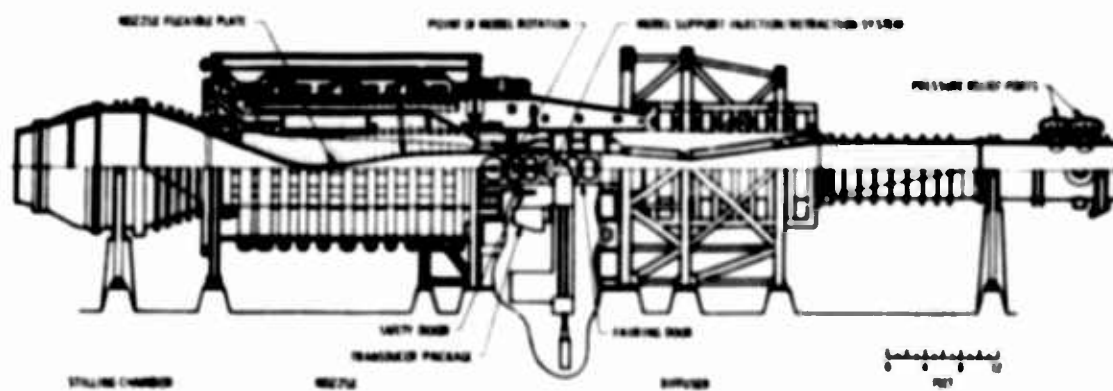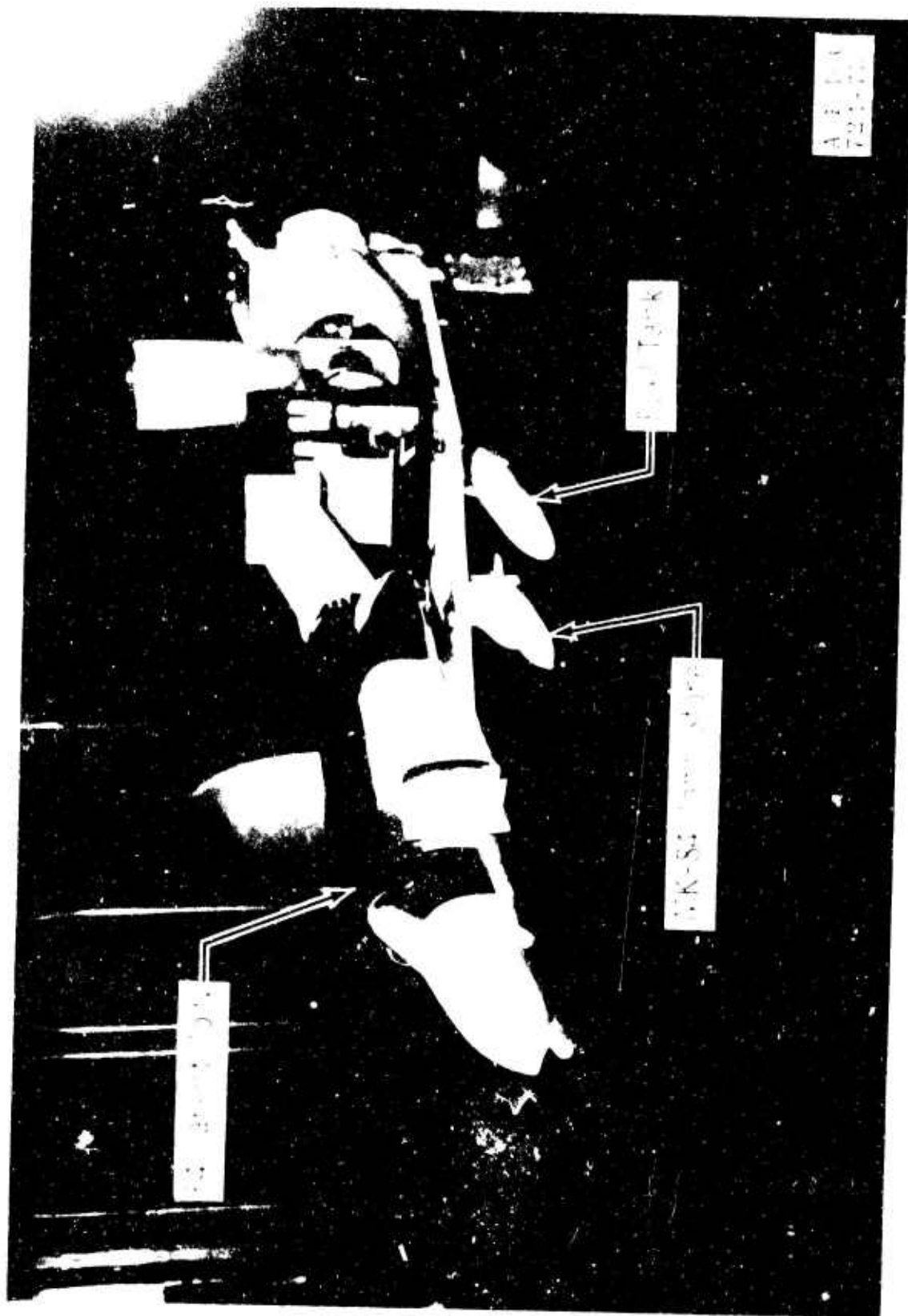
Fig. 2 Tunnel A Schematic

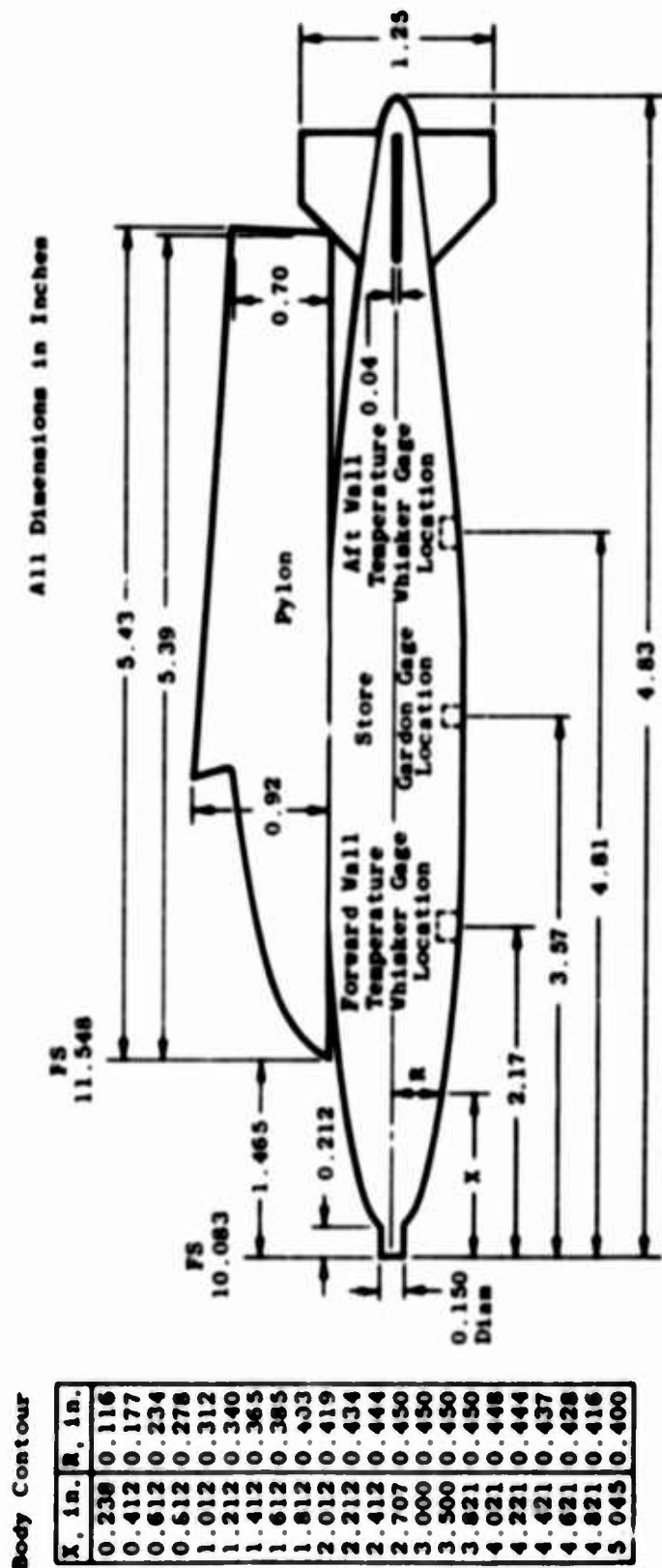Fig. 3 Installation of Parent Body, MK-84 Store, and Fuel Tank

All Dimensions in Inches

Body Contour

X, in.	R, in.
0.238	0.116
0.412	0.177
0.612	0.234
0.612	0.278
1.012	0.312
1.212	0.340
1.412	0.365
1.612	0.385
1.812	0.403
2.012	0.419
2.212	0.434
2.412	0.444
2.707	0.450
3.000	0.450
3.500	0.450
3.821	0.450
4.021	0.448
4.221	0.441
4.421	0.437
4.621	0.428
4.821	0.416
5.045	0.400

Fig. 4 MK-84 Model with Inboard Pylon and Instrumentation Locations

1 deg
MK-84 Centerline

FS
10.083

FS
10.672

BL-11.560

Fuel Tank

MK-84

BL 4.075
Centerline
Inboard Pylon

BL 6.625
Centerline
Outboard Pylon

FS
1.355

FS
0.000

BL 11.560
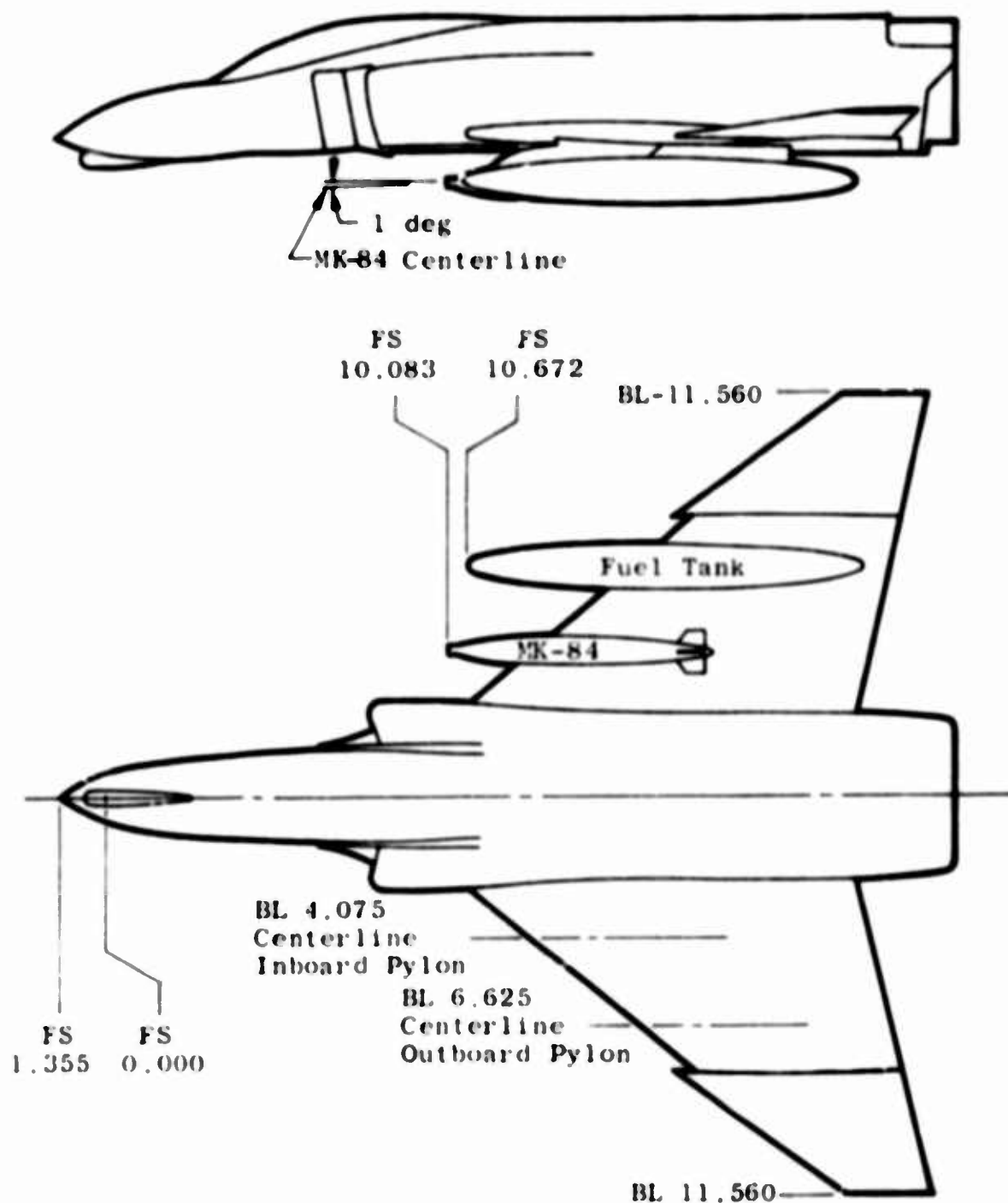
Fig. 5 Sketch Illustrating Relative Sizes of F-4C, MK-84, and Fuel Tank
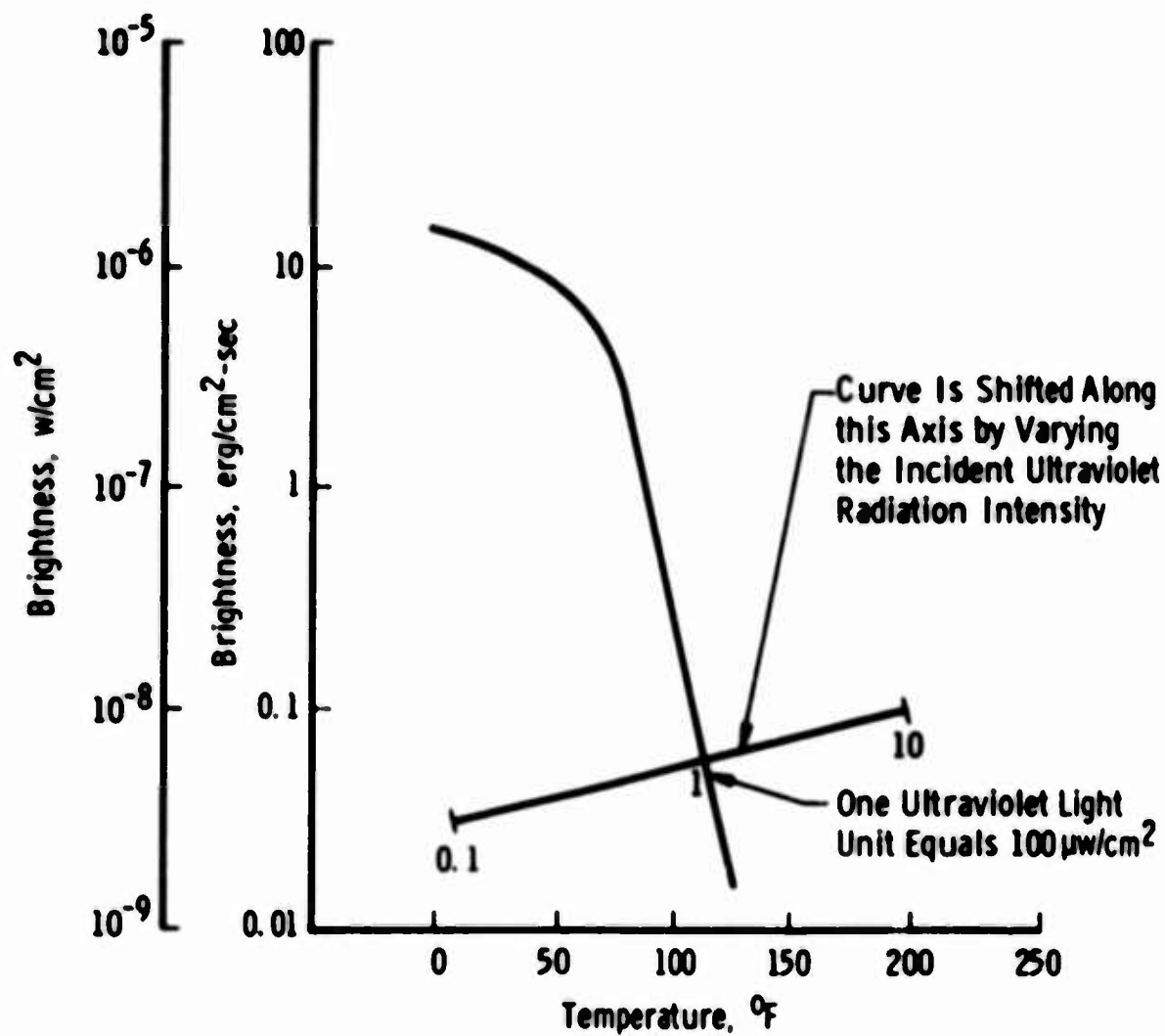
Fig. 6 Variation of Phosphor Brightness with Temperature r
U. S. Radium Randelin® 1807 Phosphor
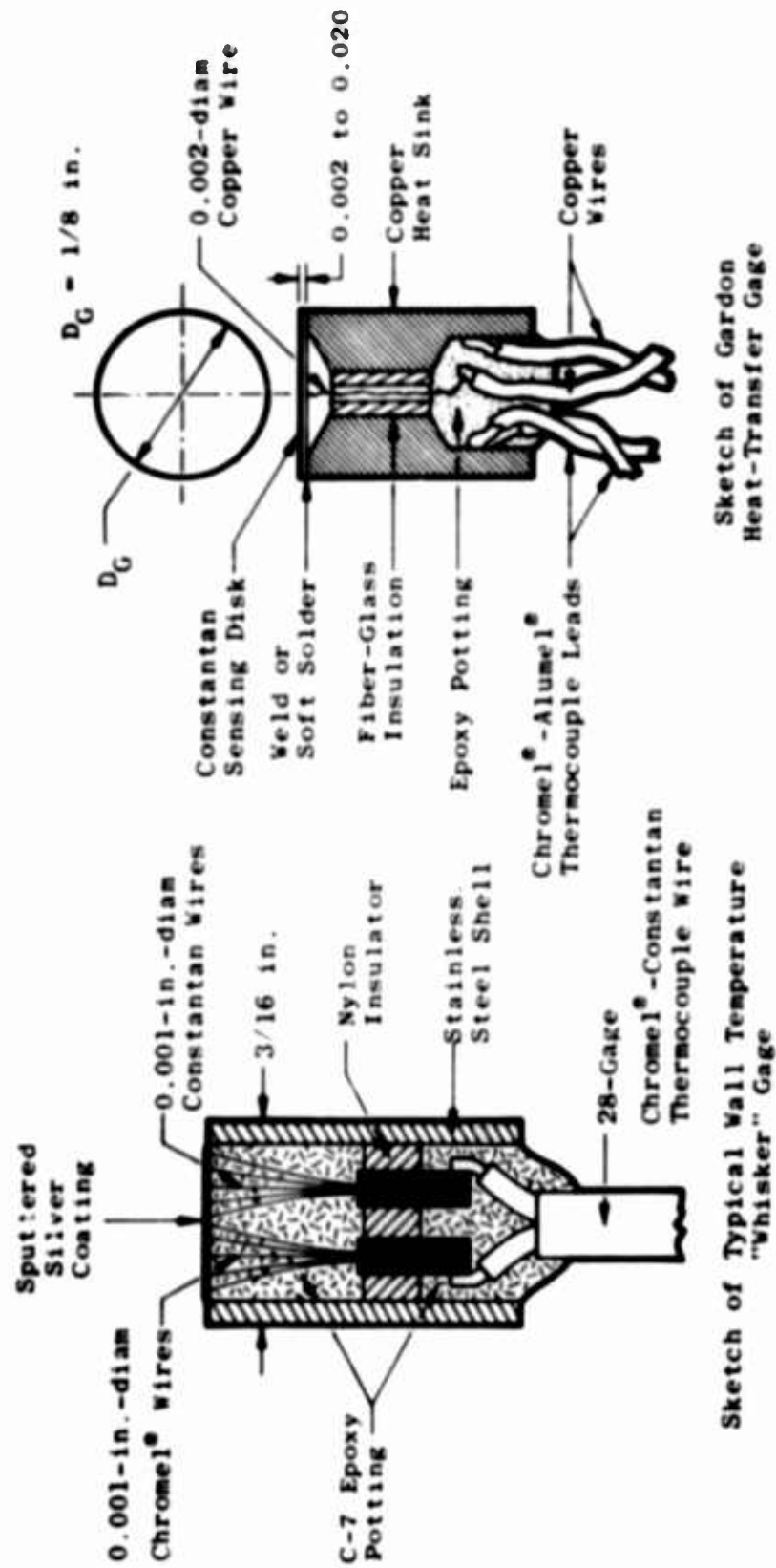
Fig. 7 Sketches of Gages That Were Installed in MK-84 Store Model

19
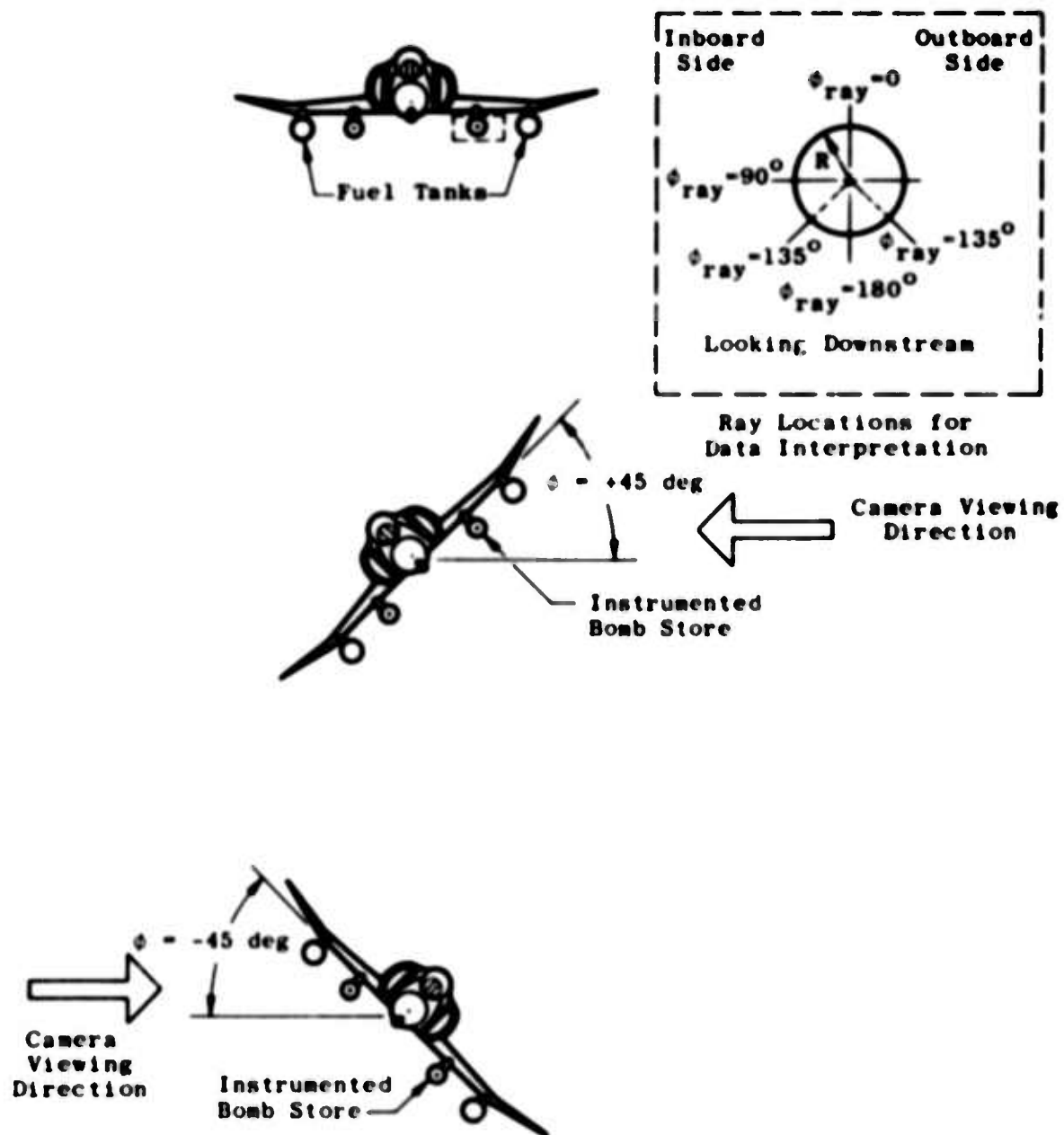
Fig. 8 Roll Positions of F-4C Parent Body for Photographic Coverage
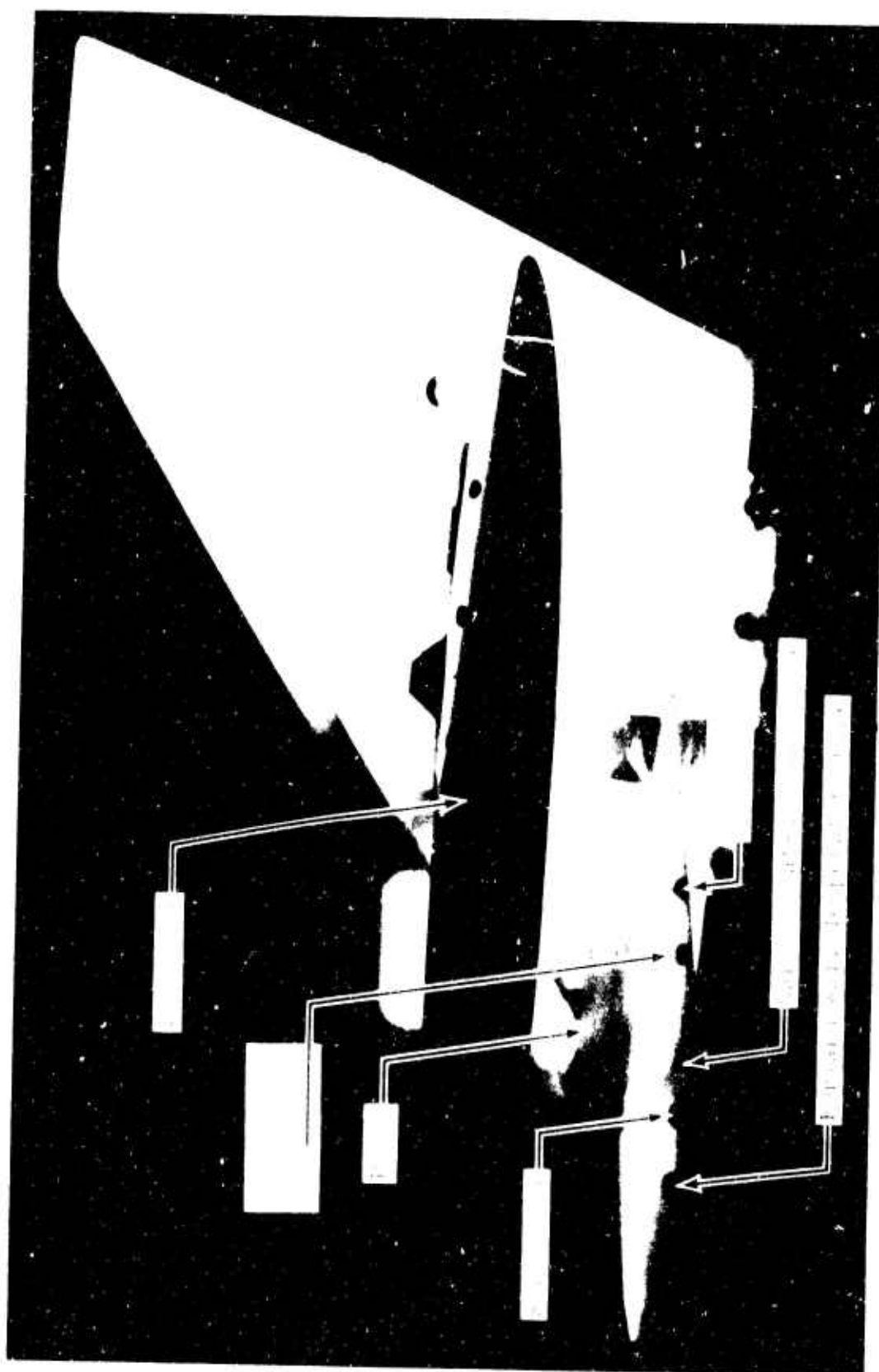
Fig. 9 Typical Black/White Picture of Phosphor Painted MK-84 Store with Parent Body Rolled +45 deg
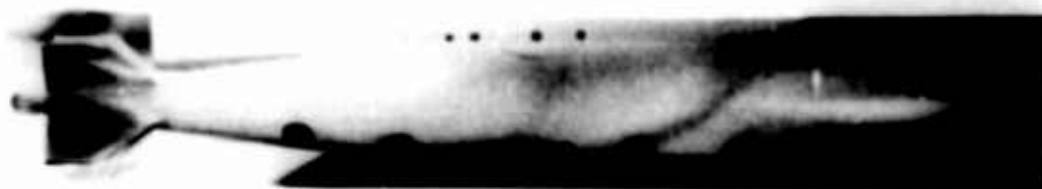
a. Black/White Photograph

Color	Wall Temperature Range, °R	h_{wt}, Btu/ft^2-hr-°F	
Lt. Green	568 - 576	22.9 - 33.4	
Dk. Green	576 - 583	33.4 - 47.9	
Orange	583 - 589	47.9 - 69.1	Crosshatching
Brown	589 - 594	69.1 - 102.1	Denotes Areas
Black	594 - 600	102.1 - 134.6	of Invalid Data

b. Datacolor (Thermographic Data) Photograph

Fig. 10 Heating Patterns on the Phosphor-Painted MK-84 Store, Inboard Side, Fuel Tanks Off, $a = 0$, $Re_\infty/ft = 3.84 \times 10^6$, $M_\infty = 1.76$

Fuel Tanks Off

Local "Hot Spot"

Fuel Tanks On

a. $M_\infty = 1.76$, $Re_\infty/ft = 3.84 \times 10^6$

Crosshatching
Denotes Areas of
Invalid Data

Increasing
Value of h_{w}

Fuel Tanks Off

Local "Hot Spot"

Fuel Tanks On

b. $M_\infty = 2.00$, $Re_\infty/ft = 4.29 \times 10^6$
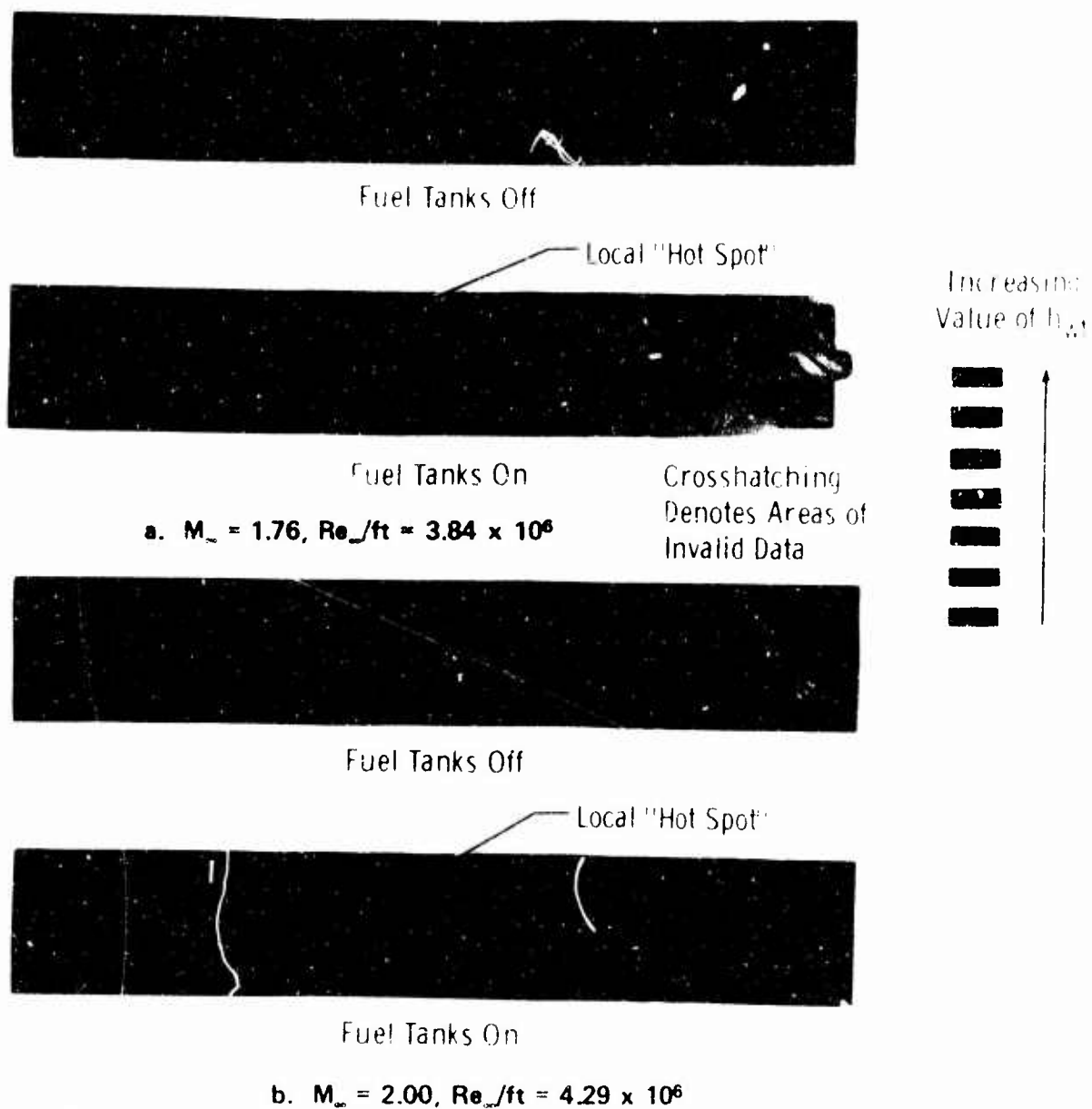
Fig. 11 Datacolor (Thermographic Data) Photographs Showing the Influence of
the Fuel Tanks, $\alpha = 0$, Outboard Side of MK-84

Preceding page blank

25
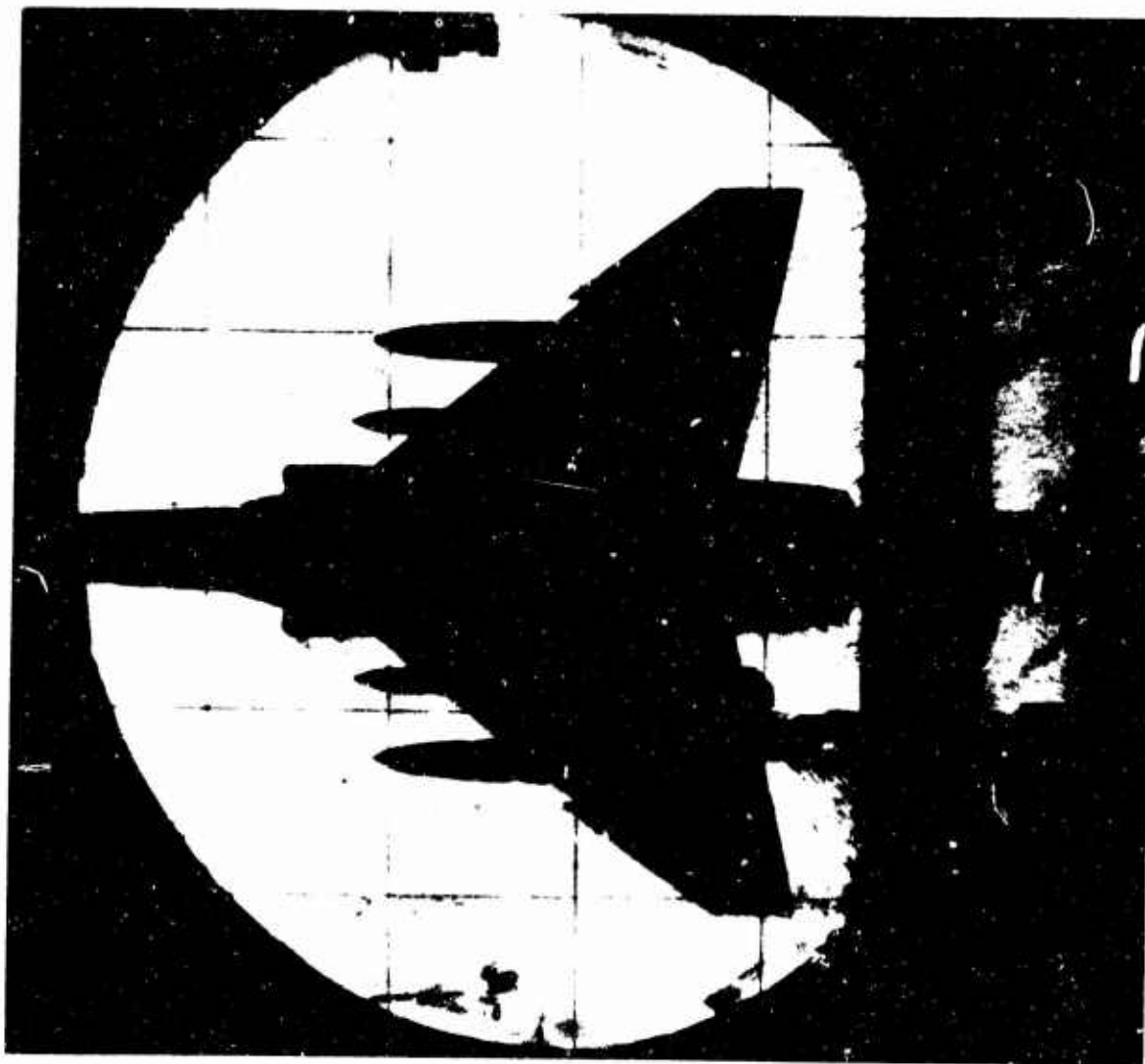
Fig. 12 Shadowgraph of Two MK 84 Stores Attached to the Wings of F-4C with Fuel Tanks, $\alpha = 0$, Re./ft $= 4.6 \times 10^6$, M $= 1.76$

Preceding page blank
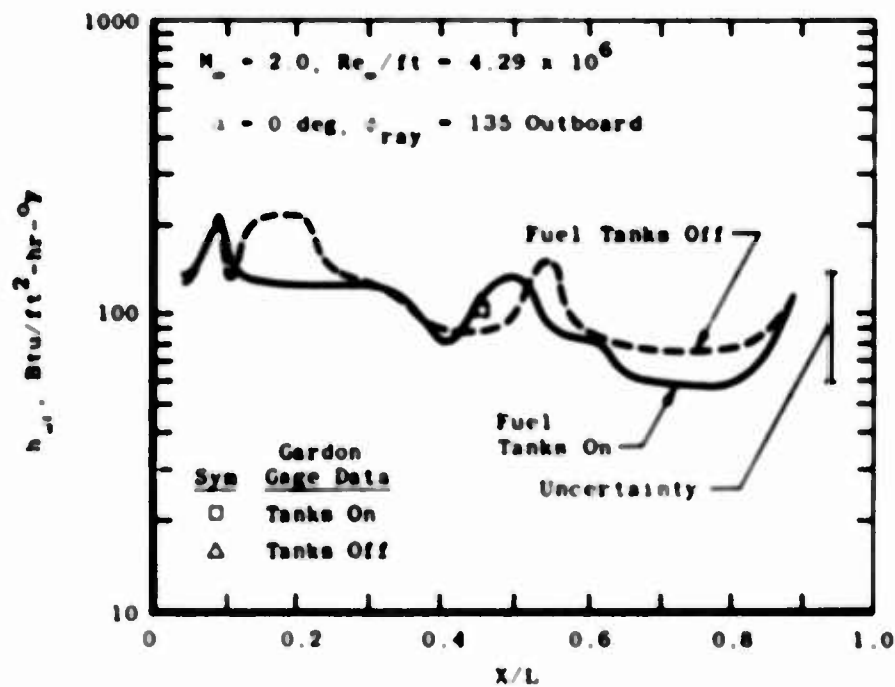
a. Outboard
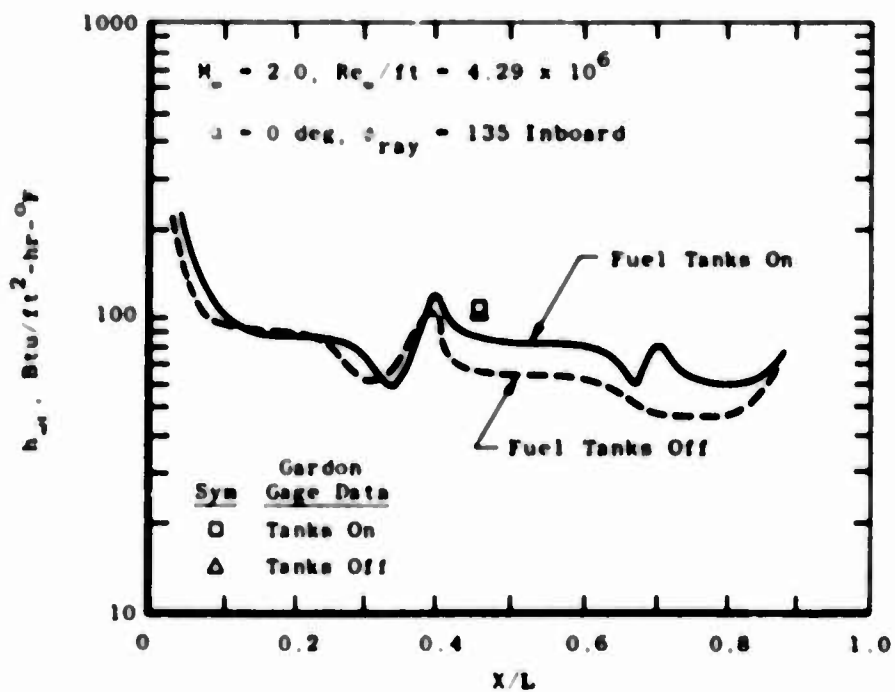
b. Inboard

Fig. 13 Influence of the Fuel Tanks on the Store Heating Distributions
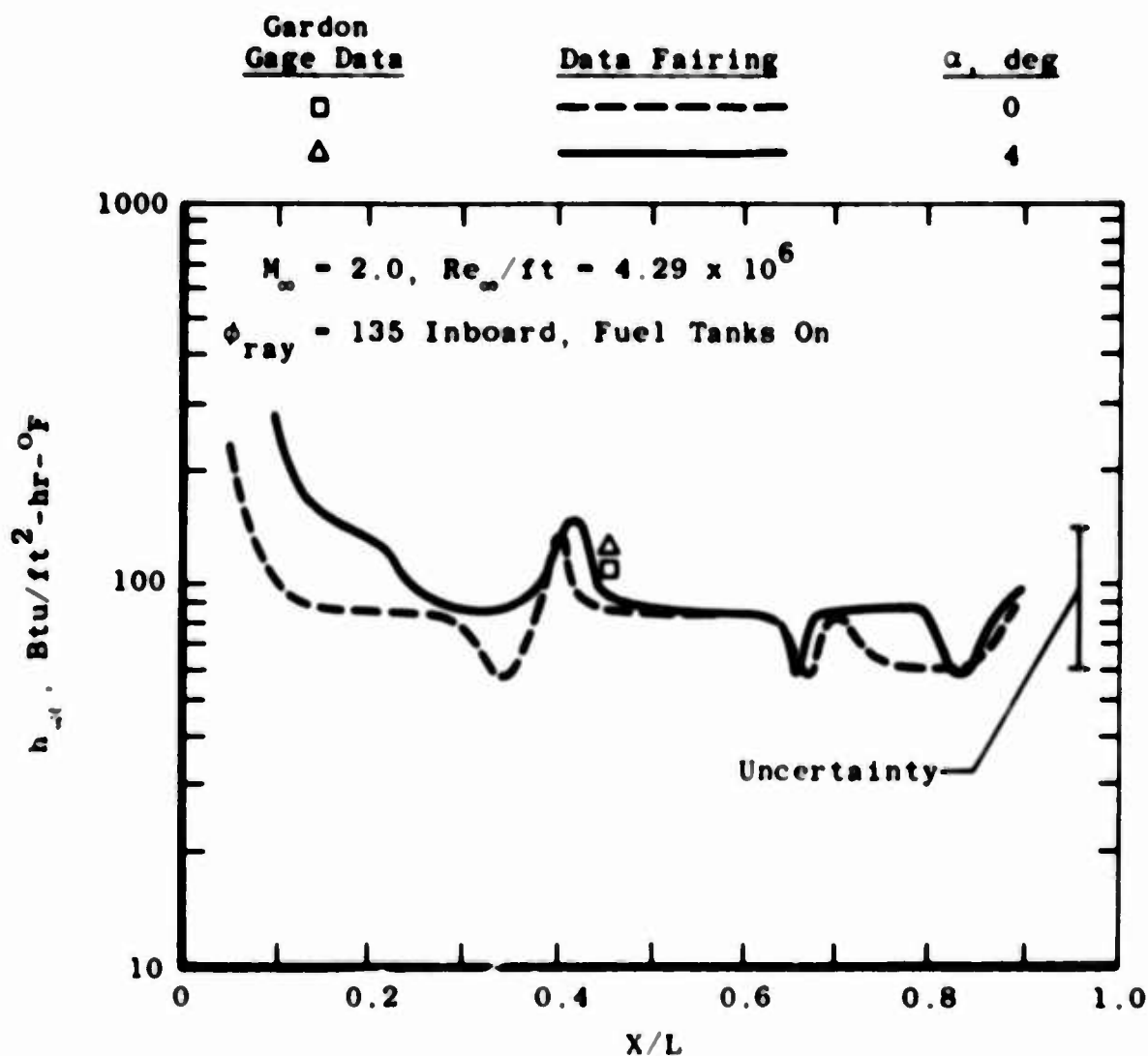
Fig. 14 Influence of Angle-of-Attack on the Heat-Transfer Coefficient Distribution
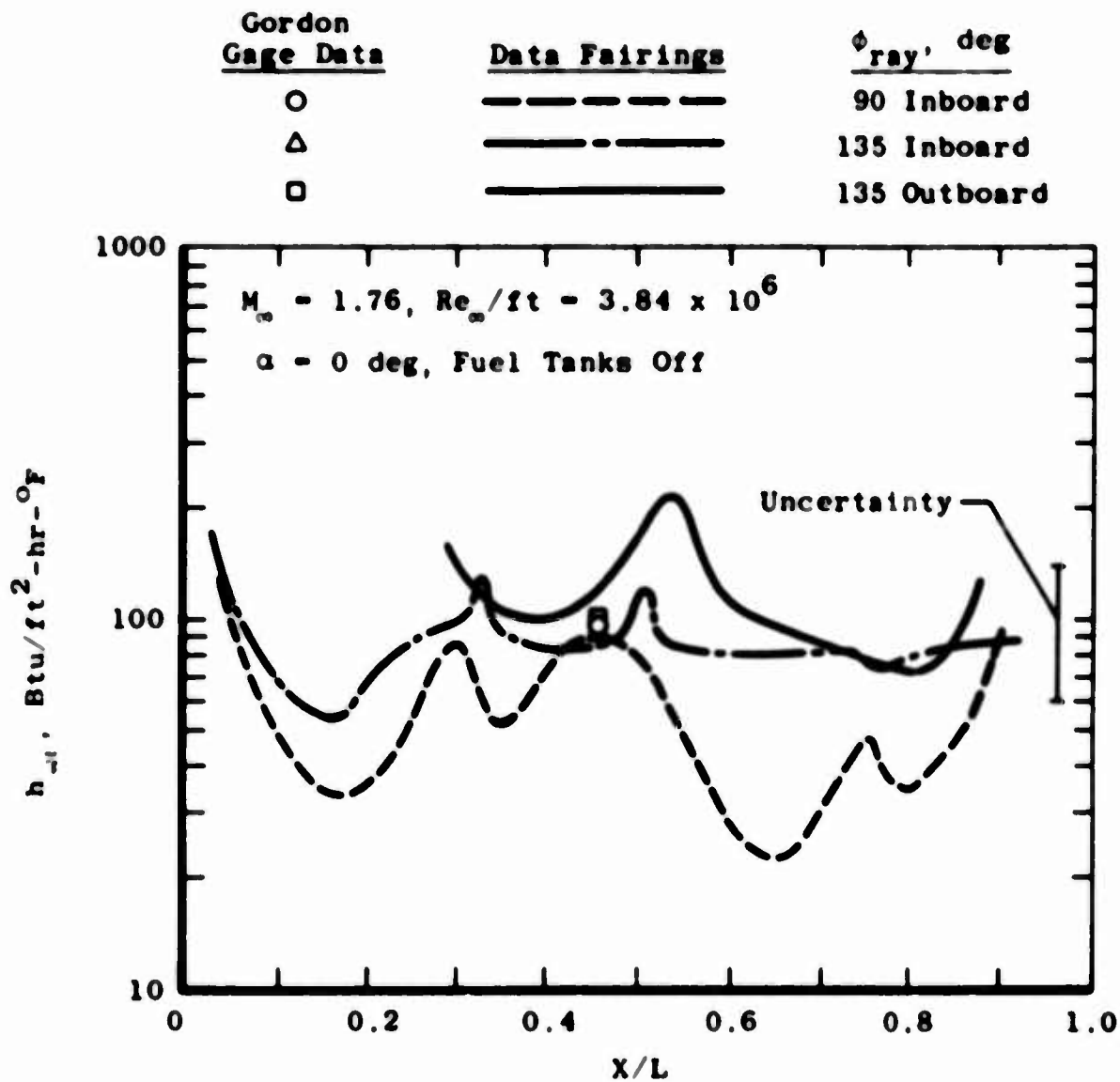
Fig. 15 Influence of Radial Position on the Axial Heat-Transfer Coefficient
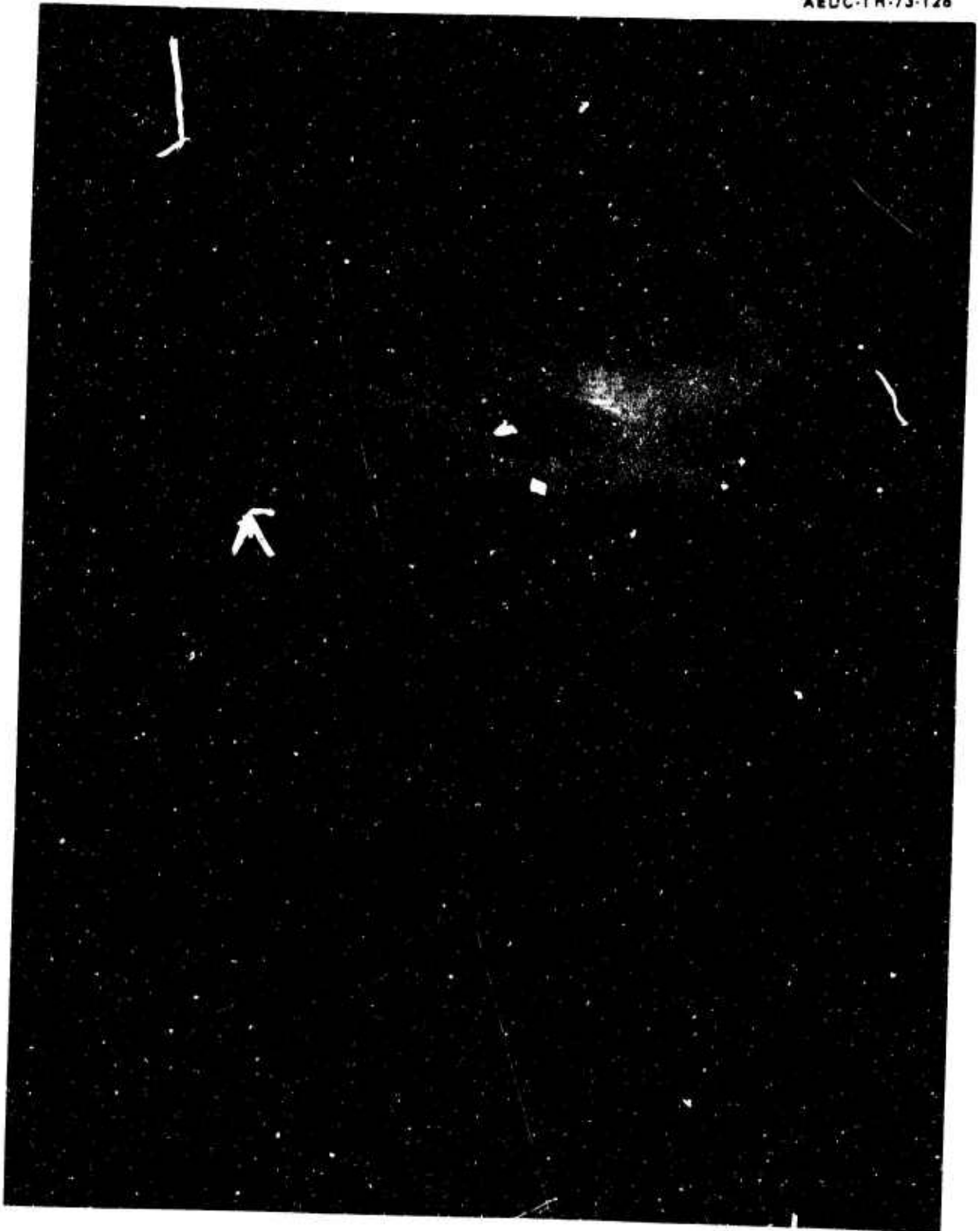Distribution on the MK-84 Store

Fig. 16 Oil Flow Patterns of Two MK-84 Stores Attached to the Wings of F-4C
with Fuel Tanks, $a = 0$, $Re_\infty/ft = 4.29 \times 10^6$, $M_\infty = 2.00$

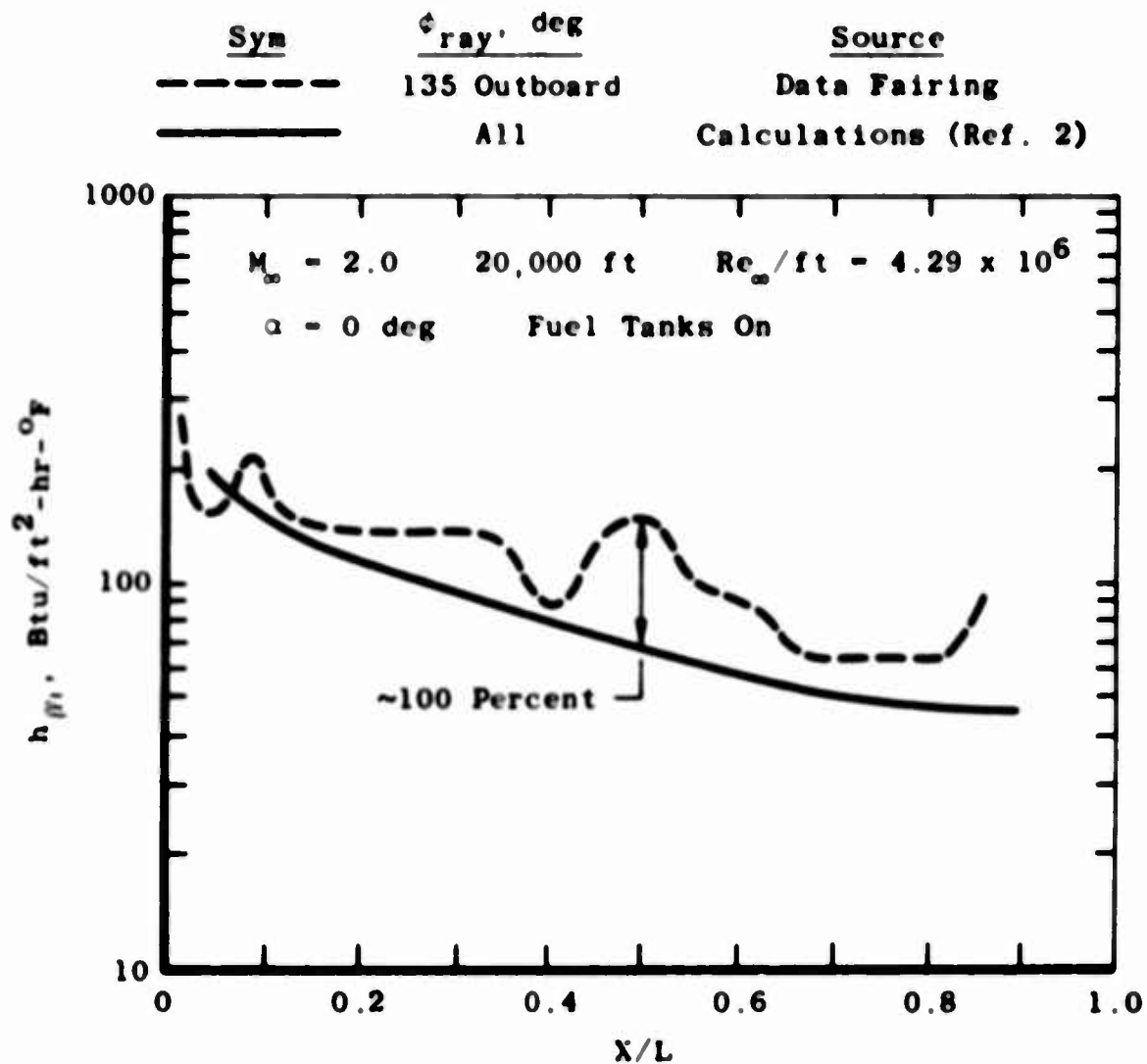Fig. 17 Schematic Showing Extrapolation of Wind Tunnel Data to Flight Conditions

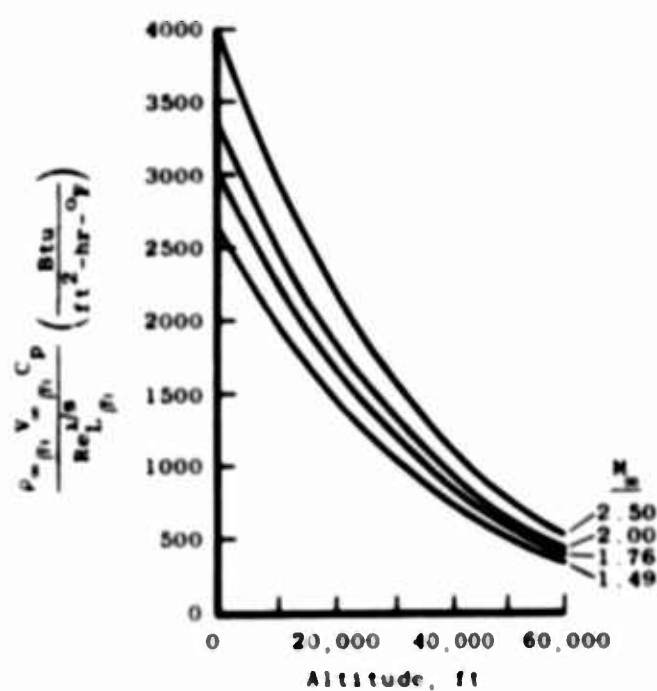**Preceding page blank**

Fig. 18 Comparison of Typical Data Fairing with Interference-Free
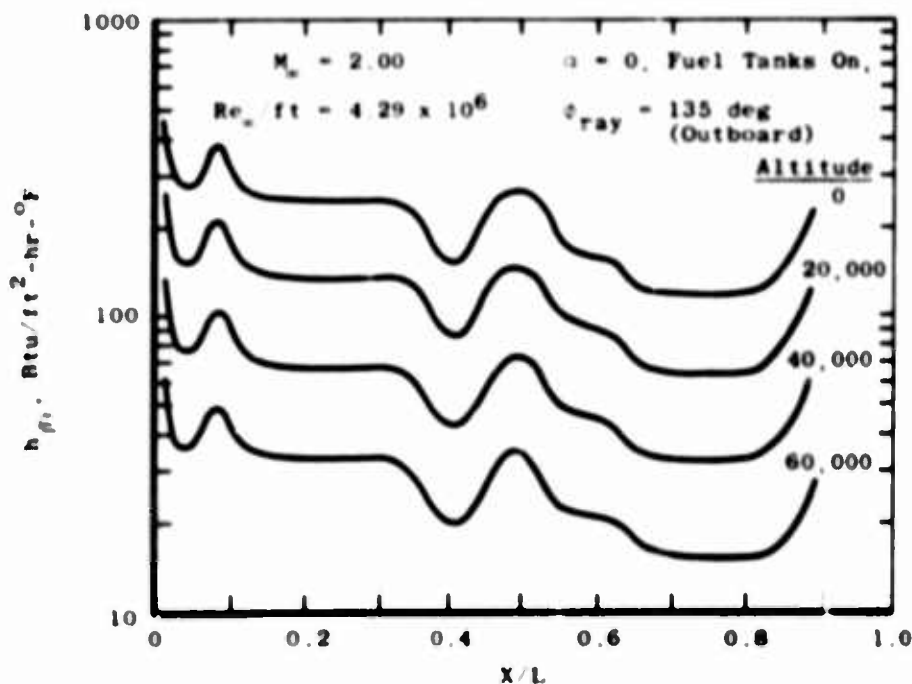Calculations Based on M_∞ = 2.00

Fig. 19 Influence of Altitude on the Heat-Transfer Coefficient Distribution
for Given Free-Stream Mach Numbers

TABLE I
TEST SUMMARY

	$M_\infty = 1.49$[*]		$M_\infty = 1.76$		$M_\infty = 2.00$[**]		$M_\infty = 2.50$	
	Configuration 1	Configuration 2	Configuration 1	Configuration 2	Configuration 1	Configuration 2	Configuration 1	Configuration 2
$\alpha = 0°$, $\phi = 0°$		x		x	x	x	x	x
$\alpha = 0°$, $\phi = +45°$		x	x	x	x	x	x	x
$\alpha = 0°$, $\phi = -45°$			x	x	x	x	x	x
$\alpha = +45°$, $\phi = +45°$			x			x		x
$\alpha = +45°$, $\phi = -45°$			x		x		x	

Configuration
1 - F4/MK-84/with fuel tanks
2 - F4/MK-84/without fuel tanks

[*]Besides the heat transfer data that were obtained at the nominal tunnel operating conditions for $M_\infty = 1.49$, 16-mm color motion pictures and heat-transfer data were taken at: $M_\infty = 1.49$, $P_o = 15$ psia, $T_o = 600°R$ for ($\phi = 0°$, $= 90°$, $180°$, $= 0°$) and ($\alpha = 0°$, $= 6°$, $6°$, $= 0°$).

[**]Zyglo oil flow data were also obtained at $M_\infty = 2.00$ for ($\alpha = 0°$, $\phi = 0°$) and ($\alpha = 0°$, $\phi = +45°$, $+90°$).